



HAL
open science

Complex population structure of the Atlantic puffin revealed by whole genome analyses

Oliver Kersten, Bastiaan Star, Deborah Leigh, Tycho Anker-Nilssen, Hallvard Strøm, Jóhannis Danielsen, Sébastien Descamps, Kjell Erikstad, Michelle Fitzsimmons, Jérôme Fort, et al.

► To cite this version:

Oliver Kersten, Bastiaan Star, Deborah Leigh, Tycho Anker-Nilssen, Hallvard Strøm, et al.. Complex population structure of the Atlantic puffin revealed by whole genome analyses. *Communications Biology*, 2021, 4 (1), 10.1038/s42003-021-02415-4 . hal-03346894

HAL Id: hal-03346894

<https://hal.science/hal-03346894v1>

Submitted on 22 Nov 2021















HAL is a multi-disciplinary open access archive for the deposit and dissemination of scientific research documents, whether they are published or not. The documents may come from teaching and research institutions in France or abroad, or from public or private research centers.

L'archive ouverte pluridisciplinaire **HAL**, est destinée au dépôt et à la diffusion de documents scientifiques de niveau recherche, publiés ou non, émanant des établissements d'enseignement et de recherche français ou étrangers, des laboratoires publics ou privés.

<https://doi.org/10.1038/s42003-021-02415-4>

OPEN

Complex population structure of the Atlantic puffin revealed by whole genome analyses

Oliver Kersten ^{1✉}, Bastiaan Star ¹, Deborah M. Leigh ², Tycho Anker-Nilssen ³, Hallvard Strøm⁴, Jóhannis Danielsen ⁵, Sébastien Descamps ⁴, Kjell E. Erikstad^{6,7}, Michelle G. Fitzsimmons ⁸, Jérôme Fort ⁹, Erpur S. Hansen ¹⁰, Mike P. Harris¹¹, Martin Irestedt ¹², Oddmund Kleven ³, Mark L. Mallory ¹³, Kjetill S. Jakobsen ¹ & Sanne Boessenkool ^{1✉}

The factors underlying gene flow and genomic population structure in vagile seabirds are notoriously difficult to understand due to their complex ecology with diverse dispersal barriers and extensive periods at sea. Yet, such understanding is vital for conservation management of seabirds that are globally declining at alarming rates. Here, we elucidate the population structure of the Atlantic puffin (*Fratercula arctica*) by assembling its reference genome and analyzing genome-wide resequencing data of 72 individuals from 12 colonies. We identify four large, genetically distinct clusters, observe isolation-by-distance between colonies within these clusters, and obtain evidence for a secondary contact zone. These observations disagree with the current taxonomy, and show that a complex set of contemporary biotic factors impede gene flow over different spatial scales. Our results highlight the power of whole genome data to reveal unexpected population structure in vagile marine seabirds and its value for seabird taxonomy, evolution and conservation.

¹Centre for Ecological and Evolutionary Synthesis (CEES), Department of Biosciences, University of Oslo, Oslo, Norway. ²WSL Swiss Federal Research Institute, Birmensdorf, Switzerland. ³Norwegian Institute for Nature Research (NINA), Trondheim, Norway. ⁴Norwegian Polar Institute, Fram Centre, Langnes, Tromsø, Norway. ⁵Faroe Marine Research Institute (FAMRI), Tórshavn, Faroe Islands. ⁶Norwegian Institute for Nature Research (NINA), Fram Centre, Langnes, Tromsø, Norway. ⁷Centre for Biodiversity Dynamics (CBD), Norwegian University of Science and Technology (NTNU), Trondheim, Norway. ⁸Environment and Climate Change Canada, Newfoundland and Labrador, Canada. ⁹Littoral, Environment et Sociétés (LIENSs), UMR 7266 CNRS—La Rochelle Université, La Rochelle, France. ¹⁰South Iceland Nature Research Centre, Ægisdaga 2, Vestmannaeyjar, Iceland. ¹¹UK Centre for Ecology & Hydrology, Penicuik, Midlothian, UK. ¹²Department of Bioinformatics and Genetics, Swedish Museum of Natural History, Stockholm, Sweden. ¹³Department of Biology, Acadia University, Wolfville, Nova Scotia, Canada. ✉email: oliver.kersten@ibv.uio.no; sanne.boessenkool@ibv.uio.no

Seabirds are important ecosystem indicators and drivers^{1–3}, and have long had an integral place in human culture and economy^{4–6}. Nevertheless, global seabird numbers have deteriorated by an alarming 70% since the mid-20th century^{7,8}. These declines pose a serious threat to marine ecosystems, human society, and culture^{7,9,10}, highlighting the importance of seabird conservation management. Within such management, the identification of distinct population units, i.e., demographically independent populations with restricted gene flow among them^{11,12}, is a fundamental first step towards optimized conservation^{11,13,14}. Defining such units is, however, difficult for many seabirds because of their complex ecology¹⁵. Detailed genomic data including thousands of loci provide new possibilities to assess levels of connectivity and gene flow between distinct breeding populations and, thus, help identify relevant conservation units for seabirds^{15,16}. Indeed, a few recent publications using reduced genomic representation approaches (e.g., RAD-seq) have reported fine-scale structure over various spatial scales^{17–21}. These studies highlight the great potential of genomic data to disentangle barriers to gene flow that would otherwise remain undetected, but remain nonetheless limited due to incomplete sampling of the genome²².

The Atlantic puffin (*Fratercula arctica*, Linnaeus, 1789, hereafter “puffin”) is an iconic seabird species, prevalent in popular culture²³, important for tourism^{24,25}, and inherently valuable for the marine ecosystem¹. Puffins were historically widely harvested for their meat and down^{6,26,27} and exploitation remains an important cultural tradition in Iceland and the Faroe Islands^{6,24}. Its breeding range stretches from the Arctic coast and islands of European Russia, Norway, Greenland, and Canada, southward to France and the USA²⁸ (Fig. 1a). Puffins have been designated as “vulnerable” to extinction globally and listed as “endangered” in Europe²⁹. Notably, the once world’s largest puffin colony (Røst, Norway) has experienced complete fledging failure during nine of the last 13 seasons and has lost nearly 80% of its breeding pairs during the last 40 years^{29–31}. Similarly, Icelandic and Faroese puffins have experienced low productivity and negative population growth since 2003³².

Puffins have been broadly classified into three taxonomic groups along a latitudinal gradient based on size, with the *smallest* found around France, Britain, Ireland and southern Norway (*F. a. grabae*), *intermediate* sized puffins around Norway, Iceland, and Canada (*F. a. arctica*) and the *largest* puffins found in the High Arctic, e.g. Spitsbergen³³, Greenland³⁴, and north-eastern Canada³⁵ (*F. a. naumanni*)³⁶ (Fig. 1a). Nevertheless, this broad classification into three subspecies has been controversial^{28,37,38} and the population structure of puffins remains unresolved at all spatial scales³⁷. This knowledge gap obstructs efforts towards an assessment of dispersal barriers, limits our understanding of cause-and-effect dynamics between population trends, ecology and the marine ecosystem, and hinders the development of adapted large-scale conservation actions.

Here, we present the, to the best of our knowledge, first whole-genome analysis of structure, gene flow, and taxonomy of a pelagic, North Atlantic seabird. We generated a de novo draft assembly for the puffin and resequenced 72 individuals across 12 colonies representing the majority of the species’ breeding range (Fig. 1a). Our work suggests that a complex interplay of ecological factors contributes to the range-wide genomic population structure of this vagile seabird.

Results

Genome assembly and population sequencing. Based on synteny with the razorbill (*Alca torda*), a total of 13,328 puffin scaffolds were placed into 26 pseudo-chromosomes, leaving 17.06

Mbp (1.4%) unplaced and yielding an assembly of 1.294 Gbp (Supplementary Data 1, Table S1). This assembly contains 4,522 of the 4,915 genes (92.0%) of complete protein-coding sequences from the avian set of the OrthoDB v9 database (Supplementary Data 1). We also assembled the puffin mitogenome (length of 17,084 bp) with a similar arrangement of genomic elements as other members within the Alcidae^{39,40} (Fig. S1, Table S2). For the 72 resequenced specimens, we analyzed a total of 5.77 billion paired reads, obtaining an average fold-coverage of 7X (range 3.0–10) for the nuclear genome and 591X (5.3–1800) for the mitochondrial genome per specimen (Fig. 1a, Supplementary Data 2). One individual (IOM001) was removed from both datasets (nuclear and mitochondrial) due to a substantially lower number of mapped reads (endogeny) relative to all other samples (Supplementary Data 2) resulting in a large proportion of missing sites (Fig. S2). Additional filtering produced a final genotype likelihood dataset of 1,093,765 polymorphic nuclear sites and 192 mitochondrial single-nucleotide polymorphisms (SNPs, Supplementary Data 3) in 71 birds (36 males and 35 females).

Genomic population structure. Genomic variation across 71 puffin mitogenomes defines 66 polymorphic haplotypes that indicate a recent global population expansion and show no significant population structure (Fig. 1b, Figs. S3, S4, Tables S3, S4). In contrast, we inferred four main population clusters using principal component analysis (PCA) of the nuclear whole-genome dataset (Fig. 1c). Puffins from Spitsbergen are most distinct, while puffins from Bjørnøya are located between Spitsbergen and a larger, central cluster consisting of populations from Norway, Iceland, and the Faroe Islands (Fig. 1c, Fig. S5a). Puffins from Canada form their own distinct cluster, as do those from the Isle of May, southeast Scotland (Fig. 1c, Fig. S5b). Hierarchical PCA analyses of the cluster comprising the mainland Norwegian, Icelandic and Faroese colonies reveal further fine-scale structure separating Norwegian (Hornøya and Røst) and Faroese/Icelandic colonies (Fig. S5c). Model-based clustering (ngsAdmix) agrees with the results from the PCA (Fig. 1d). The optimal model fit for the entire dataset is either $K=2$ or $K=4$ (Fig. S6a), as determined by the method of Evanno et al.⁴¹. At $K=2$, ngsAdmix separates Spitsbergen from the other colonies, with Bjørnøya being admixed (following separation along PCA 1), whereas at $K=4$, ngsAdmix reflects the structure of three additional distinct clusters representing Spitsbergen, Canada, the Isle of May, and a central group with more shared ancestry (Fig. 1d). The shared ancestry of the central group remains present in hierarchical admixture analyses excluding Spitsbergen and Bjørnøya individuals (Figs. S6b, S7). We find no fixed alleles and pairwise F_{ST} values between colonies and genomic clusters are low (<0.01) (Table S4), apart from any comparisons involving the Spitsbergen population, which show substantially higher F_{ST} values (0.03–0.08).

Phylogenetic reconstructions using individual-based Neighbor-Joining (NJ) and maximum likelihood (ML) methods (Fig. 2a, Fig. S8), as well as population-based analyses in Treemix (Fig. 2b), support the distinctiveness of the Spitsbergen, Canada, and the Isle of May puffins with each group forming monophyletic clades with 100% bootstrap support. In contrast, Bjørnøya forms a paraphyletic clade between Spitsbergen and northern Norway (Fig. 2a). The population clusters identified by the PCA and ngsAdmix at smaller spatial scales are also identified in the topologies of the NJ and ML trees, sorting individuals predominantly according to geographical location, although with low bootstrap support (>80) due to large inter-individual variability (Fig. 2a, Fig. S7). Allowing a single migration edge in the Treemix phylogeny identifies recent gene flow from

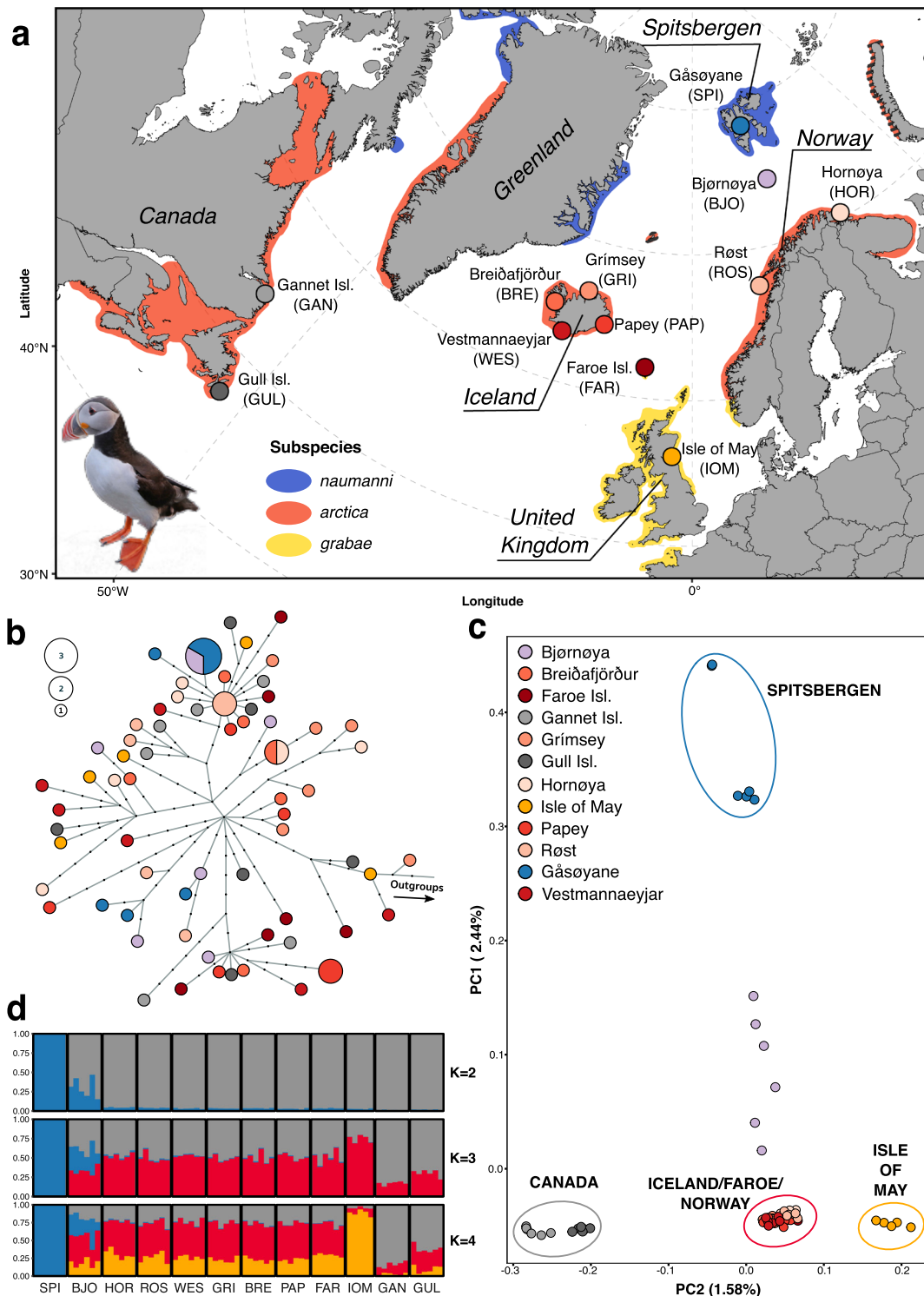


Fig. 1 Sampling distribution and genomic structure of 71 Atlantic puffin individuals across 12 colonies throughout the breeding range. a Map presenting the location of the 12 sampling sites. Color shading indicates the breeding range of the species as a whole, as well as the recognized subspecies. **b** Mitochondrial haplotype network based on a maximum likelihood tree generated with IQTree and visualized using Fitchi. It contains 66 unique haplotypes identified by 192 mitogenome-wide SNPs. Sizes of circles are proportional to haplotype abundance. Color legend is provided in (c). Black dots represent inferred haplotypes that were not found in the present sampling. **c** Principal component analysis (PCA) using genotype likelihoods at 1,093,765 polymorphic nuclear sites calculated in ANGSD to project the 71 individuals onto PC axes 1 and 2. Each circle represents a sample and colors indicate the different colonies. The percentage indicates the proportion of genomic variation explained by each axis. The color coding of the colonies is consistently used throughout the manuscript. **d** CLUMPAK-averaged admixture plots of the best K's using the same genotype likelihood panel as in (c). Each column represents a sample and colonies are separated by solid white lines. Optimal K's were determined by the method of Evanno et al.⁴¹ (see Fig. S6a) and colors indicate the ancestry fraction to the different clusters. The dataset(s) needed to create this figure can be found at <https://doi.org/10.6084/m9.figshare.14743242.v1>.

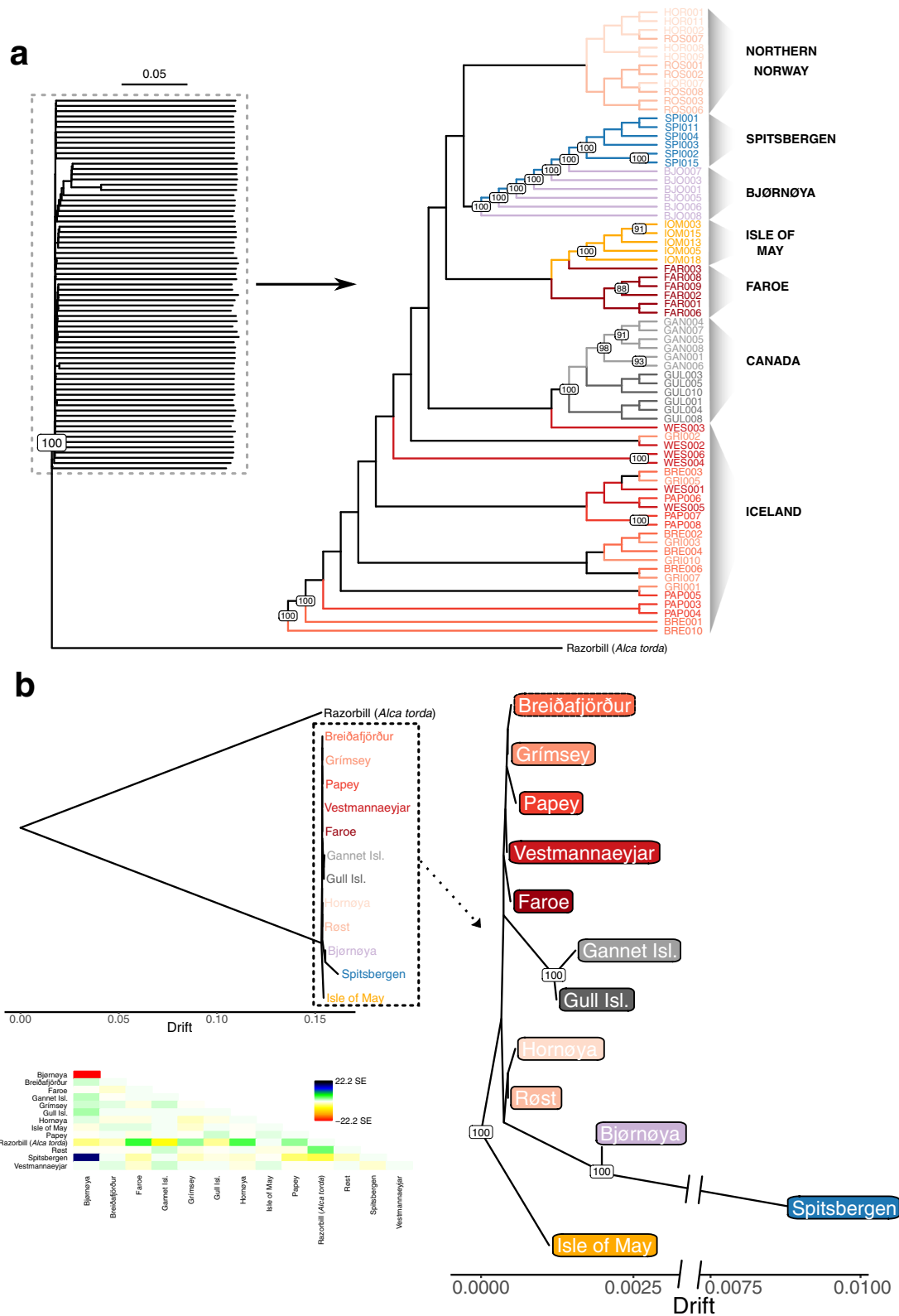


Fig. 2 Phylogenetic reconstruction of individual and colony relationships from 71 Atlantic puffin individuals sampled across 12 colonies throughout the species' breeding range. **a** An individual-based neighbor-joining tree constructed using pairwise p-distances calculated from genotype likelihoods at 1,093,765 polymorphic nuclear sites. Branch lengths and the outgroup were removed for the zoomed-in section to improve visualization. **b** A population-based maximum likelihood Treemix analysis using allele frequencies at the same 1,093,765 polymorphic nuclear sites as in **(a)**. Both trees are rooted using the razorbill as an outgroup. The tree in **(b)** is visualized with and without the outgroup. Branch lengths are equivalent to a genetic drift parameter. The heatmap indicates the residual fit of the tree displaying the standard error of the covariance between populations. In **(a)** and **(b)**, the color coding of the colonies is consistent with those in Fig. 1 and node labels show bootstrap support >80. The dataset(s) needed to create this Figure can be found at <https://doi.org/10.6084/m9.figshare.14743299.v1>.

Spitsbergen to Bjørnøya (likelihood = 792.106; Figs. S9, S10a). Adding additional migration edges to the population-based ML tree does not improve the model fit and such edges are therefore not further interpreted (Figs. S9–S11).

Genetic diversity, heterozygosity, and inbreeding. Tajima's D does not significantly deviate from neutral expectation per colony (Table S3). Nucleotide diversity (π) of puffins is significantly different between colonies, with the Spitsbergen population having significantly lower nucleotide diversity than the global median (Wilcoxon Rank Sum test, $U = 4824$, $n_{\text{SPI}} = 25$, $n_{\text{Global}} = 300$, $P = 0.017$, Table S3). Colonies also differ significantly in levels of heterozygosity (Kruskal–Wallis test, $n = 12$, $P = 1 \times 10^{-6}$; Fig. 3a) and inbreeding (Kruskal–Wallis test, $n = 12$, $P = 1 \times 10^{-7}$, Fig. 3b), whereby individual inbreeding (F_{RoH}) was approximated based on runs of homozygosity (RoH)⁴². Again, the Spitsbergen colony has significantly lower levels of heterozygosity (0.00220–0.00223) and significantly higher levels of F_{RoH} values (0.161–0.172), compared to the Faroese and Icelandic colonies (Dunn test with Holm correction, $P < 0.05$, $n_1 = 6$, $n_2 = 6$). The Faroese and Icelandic colonies contain the highest levels of heterozygosity and lowest F_{RoH} values (Figs. 3a, b, Fig. S12) overall. The remaining colonies display intermediate levels (Fig. 3a, b), although heterozygosity is significantly lower (Fig. 3a, Fig. S12) and inbreeding is significantly higher (Fig. 3b, Fig. S12) on Gull Island and Bjørnøya compared to the Icelandic and Faroese colonies (Dunn test with Holm correction, $P < 0.05$, $n_1 = 6$, $n_2 = 6$). Moreover, Spitsbergen harbors the most (an average of 718 per individual) and longest RoHs with eight being ≥ 2.3 Mbp long ($4.21 \pm 3.02\%$ of respective chromosome), whereas none of the RoHs in the remaining colonies are > 2.15 Mbp long (Fig. 3c). The only exception is a 9.65 Mbp long RoH on pseudo-chromosome 7 (18% of chromosome length) in an Isle of May individual (Fig. 3c).

Patterns of gene flow and isolation-by-distance (IBD). We investigated patterns of gene flow and IBD between the colonies using two-dimensional estimated effective migration surface (EEMS) analyses⁴³. Levels of gene flow between the Icelandic and Faroese colonies and within the Canadian group is high (3–10 \times higher than the global average), while intermediate between the Norwegian mainland colonies (around the global average). In contrast, the Spitsbergen colony is split from the remaining colonies by migration rates up to 100 \times lower than the global average (Fig. 4a, Fig. S13), while additional regions of low gene flow (2–3 \times lower than the global average) separate the Isle of May, Canadian, and Bjørnøya colonies from the rest (Fig. 4a, Fig. S13). Geographic distance between all puffin colonies is a poor predictor of pairwise genetic distance, driven by high Slatkin's linearized F_{ST} values between Spitsbergen and the other colonies (Tables S5, S6, Fig. S14). Nevertheless, the geographic distance among a subset of puffin colonies is significantly associated with genetic distance as shown by Mantel tests, linear regression model analyses, and distance-based Redundancy Analysis (dbrDA) models (Fig. 4b, Fig. S14, Tables S5, S6). Specifically, by progressively removing the more distant colonies (Spitsbergen, Isle of May, Bjørnøya, Canada), which are characterized by high Slatkin's linearized F_{ST} values at relatively small geographic distances (Fig. S14), the fit of a linear IBD model is significantly improved and the proportion of variance of genetic dissimilarity explained by geographic distance is more than doubled (Spitsbergen removed: 37.58%; Spitsbergen/Isle of May/Bjørnøya/Gannet Isl. removed: 84.98%) (Fig. 4b, Fig. S14, Table S5). Similarly, the proportion of explained genetic variance by spatial features estimated in global dbrDA models is more

than tripled (All colonies = 18.76%, Spitsbergen/Isle of May/Bjørnøya removed = 59.87%) (Table S5). In all optimized dbrDA models, geographic variables (IBD) contribute significantly to the genetic divergence, while the contribution of the mean sea surface temperature (isolation-by-environment, IBE) is minimal. IBE is only once significantly contributing to the observed genetic variance (when Spitsbergen was removed), yet accounts for less than half of the observed genetic variance (11.37%) compared to the geographic distance (28.66%) (Table S6).

Admixture on Bjørnøya. We specifically tested for patterns of admixture in Bjørnøya. Significantly negative f_3 statistics (Z score < -3) are found for all unique combinations of the phylogeny (Spitsbergen, X; Bjørnøya) (Table S7), indicating an admixed colony on Bjørnøya caused by gene flow between Spitsbergen and the remaining colonies. Similarly, significantly positive D -statistics (Z score > 3) caused by an excess of ABBA sites reveal excessive allele sharing between Spitsbergen and Bjørnøya (Fig. S15a). The close association and gene flow from Spitsbergen to Bjørnøya is further confirmed by D -statistics not being significantly different from 0 for the ((Bjørnøya, Spitsbergen), H3), Razorbill) topology (Fig. S15b).

Genetic differentiation. We assessed genome-wide patterns of genetic differentiation by calculating pairwise F_{ST} between the four genomic clusters in 50 kb sliding windows. These analyses show that the differentiation between the clusters is driven by increased F_{ST} in windows across the entire genome, including the presence of several smaller regions with elevated F_{ST} (Fig. S16). Several of these elevated F_{ST} regions are present in all pairwise comparisons (Fig. S16), whereas others are specific for certain comparisons, and may be indicative of local adaptation (Fig. S16).

Discussion

Barriers to gene flow leading to population structure are notoriously difficult to identify and remain largely unknown for most seabirds^{15,44}. Using whole-genome analyses, we here provide insights into the genetic structure of the Atlantic puffin. First, we identify four main puffin population clusters consisting of (1) Spitsbergen (High Arctic), (2) Canada, (3) Isle of May, and (4) multiple colonies in Iceland, the Faroe Islands, and Norway. Second, we find that within such clusters, genetic differentiation is driven by IBD. Finally, we find evidence for secondary contact between two clusters. These observations show that a complex set of drivers impacts gene flow over different spatial scales (100–1000s of km) between these clusters and the colonies within. In particular, the interplay between overwintering grounds, philopatry, natal dispersal, geographic distance, and potentially ocean regimes appears to explain the genomic differentiation between puffin colonies⁴⁵.

Mature puffins rarely, if ever, change their colonies, resulting in very high colony fidelity once they start breeding²⁸. Immatures, however, have been observed to visit other nearby colonies during the summer and may breed in non-natal colonies^{28,46}. Nevertheless, data on natal philopatry remain scarce, but existing evidence shows rates vary greatly (38–92%) between colonies^{28,46}. If either breeding or natal philopatry alone drive the puffin population structure, each colony should constitute its own distinct genomic entity and substantial genomic differentiation across the puffin's entire breeding range would be observed. Yet, philopatry alone cannot explain the presence of the four large-scale population clusters we observe here. Additional factors must therefore promote the distinctiveness of the four clusters. For instance, the Isle of May birds have a largely separate overwintering distribution mainly in the North Sea (Fig. S17)^{28,38,47}. Such potential

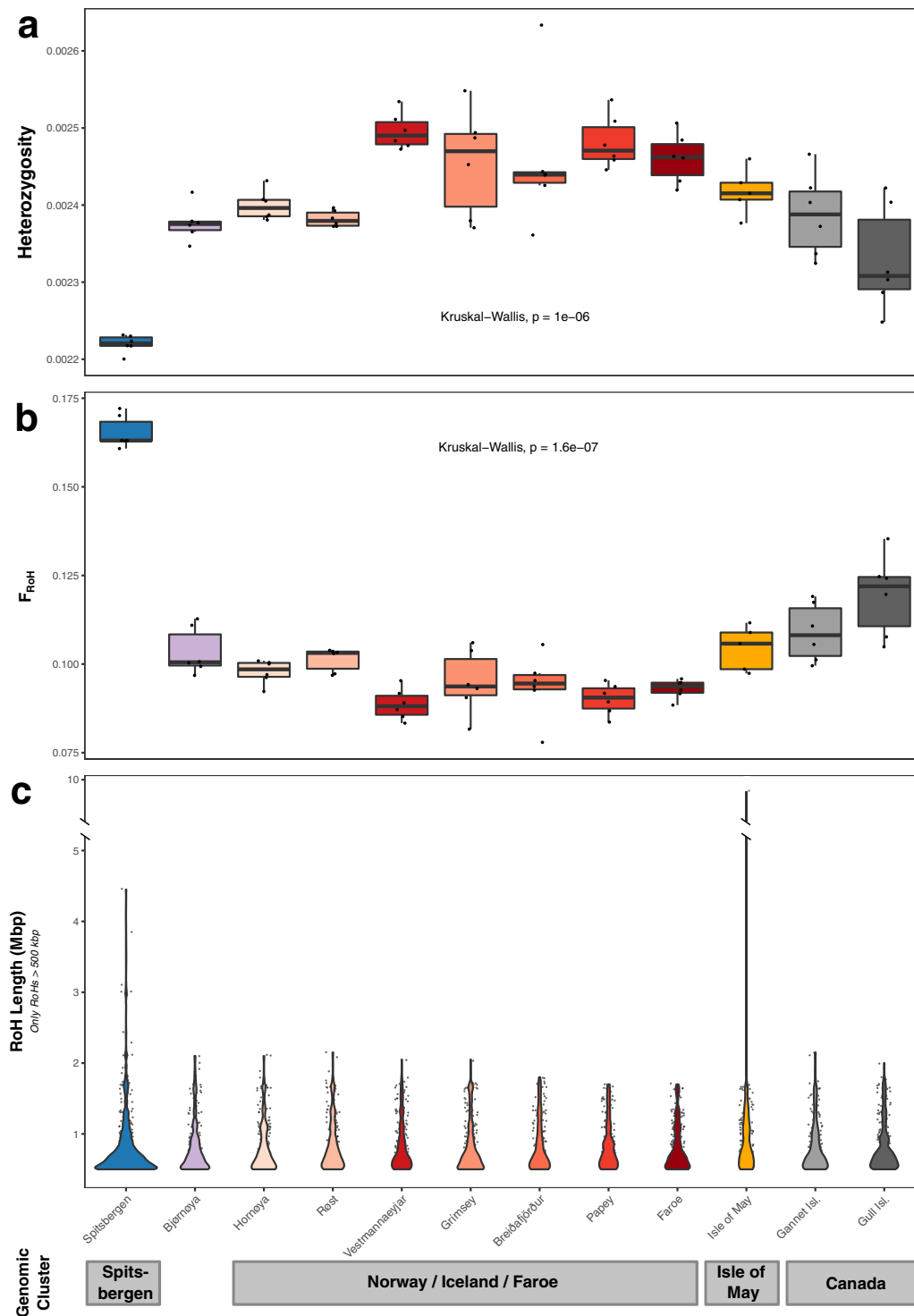


Fig. 3 Genome-wide heterozygosity, inbreeding, and Runs-of-Homozygosity (RoH) compared between 12 Atlantic puffin colonies across the species' breeding range. **a** Estimates of individual genome-wide heterozygosity based on the per-sample one-dimensional Site Frequency Spectrum calculated in ANGSD. **b** Individual inbreeding coefficients, F_{RoH} , defined as the fraction of the individual genomes falling into RoHs of a minimum length of 150 kb. RoHs were declared as all regions with at least two subsequent 100 kb windows harboring a heterozygosity below 1.435663×10^{-3} . **c** RoH length distribution across the 12 colonies only including RoHs longer than 500 kb. A single 9.65 Mbp long RoH on pseudo-chromosome 7 in an Isle of May individual required to introduce a break in the y-axis. In **(a)** and **(b)**, black dots indicate individual sample estimates and black lines the median per colony, while in **(c)**, black dots represent single RoHs. Statistical significance of differences in heterozygosity and F_{RoH} between populations was assessed with a global Kruskal-Wallis test ($n = 12$). The results of post hoc Dunn tests with Holm corrections are presented in Fig. S12. Error bars show range of values within 1.5 times the interquartile range. Different colonies in all three plots are indicated using the same color code as in Fig. 1. The dataset(s) needed to create this figure can be found at <https://doi.org/10.6084/m9.figshare.14743317.v1>.

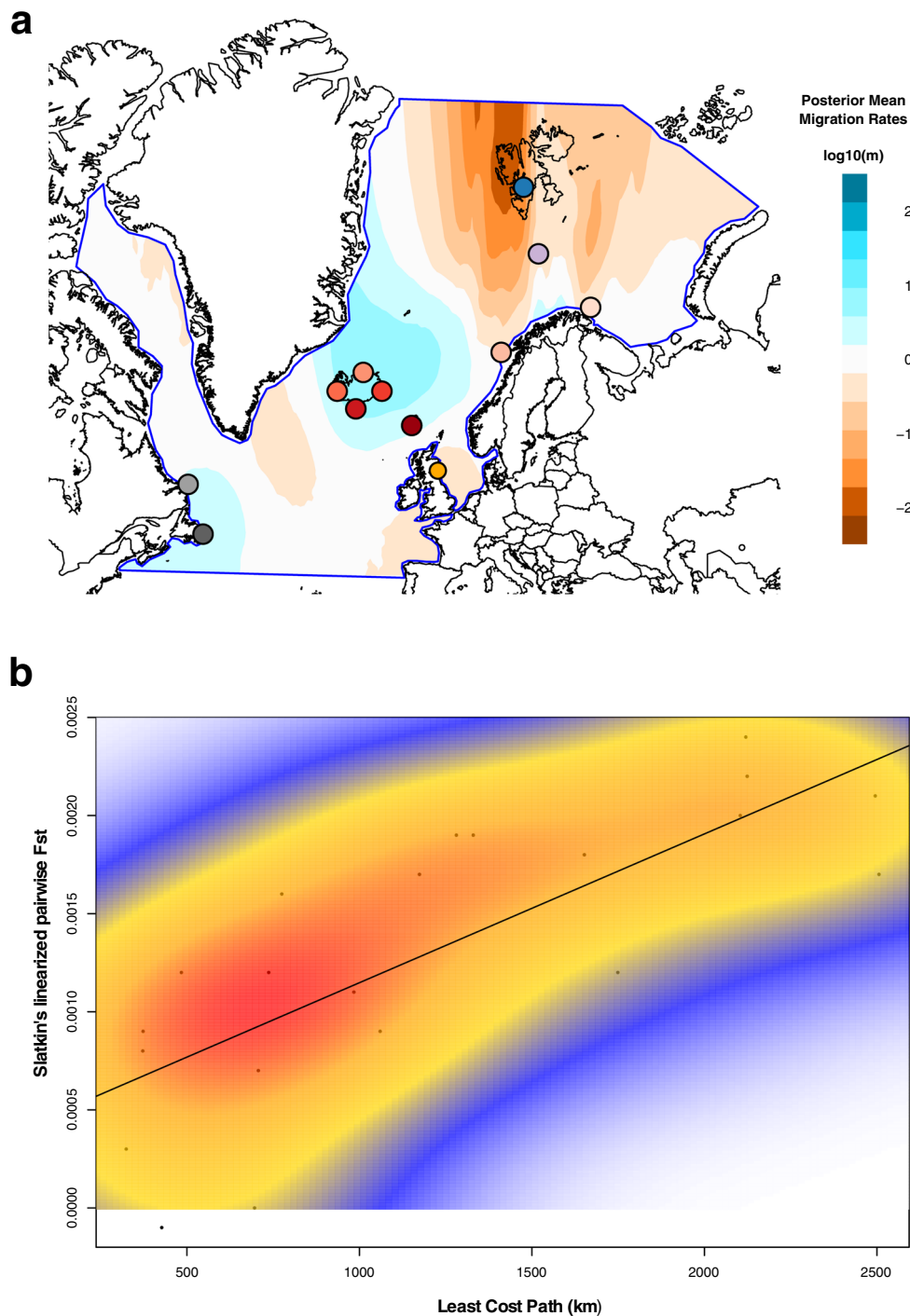


Fig. 4 Estimates of continuous long-distance gene flow and isolation by distance (IBD) across the breeding range of the Atlantic puffin estimated from 71 individuals across 12 colonies. **a** Effective migration surfaces inferred by the program EEMS using the average distance between pairs of individuals calculated in ANGSD by sampling the consensus base for each individual at 1,093,765 polymorphic nuclear sites. Darker reds indicate reduced migration across those areas, while darker blues highlight higher migration rates than the global mean. Different colonies are indicated using colors consistent with those in Fig. 1. **b** Correlation between genetic (Slatkin's linearized F_{ST}) and geographic (Least Cost Path—only over water) distance presented after removing the Spitsbergen, Bjørnøya, Isle of May, and Canadian individuals. The diagonal line visualizes the result of the multiple regression on distance matrices (MRM) analysis (slope and y-intercept). The Mantel test between genetic and geographic distance ($R = 0.775$, $P = 0.012$, $n_{Colonies} = 7$) was significant and 60.08% of the variance in Slatkin's linearized F_{ST} was explained by geographic distance (regression coefficient of linear IBD model = 0.76×10^{-6} , $P = 0.006$, $n_{Colonies} = 7$). A two-dimensional kernel density estimation (kde2d) highlights dense groups of data points, thus substructure in the genomic landscape pattern. Analyses were conducted and results visualized in R using the *ecodist*, *marmap* and *MASS* packages. The dataset(s) needed to create this figure can be found at <https://doi.org/10.6084/m9.figshare.14743323>.

geographical separation during the winter season might limit the likelihood of immatures intermixing between the Isle of May and other colonies. Similarly, distinct overwintering distributions have been found to lead to increased genetic diversification in other philopatric seabird species^{15,44,45}, such as the thick-billed murre (*Uria lomvia*)²¹ and black-browed albatross (*Thalassarche melanophris*)⁴⁸. The presence of a Canadian cluster can also be largely explained by their winter distribution around Newfoundland^{47,49}. There is, however, some fragmentary overlap in the overwintering distribution of the Canadian and Icelandic colonies off southwestern Greenland^{47,49}, suggesting that barriers to dispersal of immatures and gene flow in the western Atlantic may be further enforced by the large geographic distance. In contrast, the winter distribution from the colonies in Iceland, Norway, and the Faroe Islands overlaps off the coast of southern Greenland (Fig. S17)⁴⁷. This shared overwintering area, combined with the tendency to return to the natal colony and immature visits to nearby (up to 100 km) colonies during the summer, appears to drive a pattern of IBD among colonies (Fig. 3b). Indeed, IBD has previously been recognized as an important driver of genomic structure in seabirds, for instance in the little auk (*Alle alle*)⁵⁰ and band-rumped storm-petrel (*Oceanodroma castro*)⁵¹. While these illustrated mechanisms provide reasonable explanations for the observed dispersal barriers and population structure based on our current knowledge, validation requires additional evidence, specifically on the winter distribution of immature puffins and natal dispersal rates across colonies covering the entirety of the puffin's breeding range.

High Arctic puffins from Spitsbergen are genetically the most divergent group within our dataset harboring the highest genome-wide differentiation. They are also characterized by significantly lower levels of genetic diversity, greater inbreeding coefficients, and longer and more abundant RoHs compared to other colonies. These observations may either result from a historical bottleneck followed by isolation (e.g., founder effect), local adaptation to their extreme environment, or generally lower effective population sizes. Population abundance estimates of <10,000 breeding pairs on Spitsbergen compared to 500,000 in the West Atlantic, two million on Iceland and more than two million in the boreal East Atlantic potentially indicate a lower effective population size²⁸. The High Arctic puffins exclusively inhabit harsh, cold-current environments year-round, as they likely stay in an area bounded by the East Greenland ice edge, a latitudinal border at 70° N, and the front between the Barents and Greenland Sea during winter (Fig. S17). They are also substantially larger than birds from lower latitudes^{28,33,34}, following Bergmann's⁵² or James's⁵³ rule, as has been observed in other seabirds^{54,55}. This matches the clinal size variation of puffins that closely tracks sea temperatures in their breeding areas⁵⁶. Despite these distinctions, we find that the relatively small population of puffins on Bjørnøya (<1000 pairs²⁸), midway between Spitsbergen and mainland Norway, represents an area of secondary contact between the puffins from the High Arctic and other puffin colonies. Based on D- and f_3 -statistics, the most likely southern sources are Iceland, the Faroe Islands, Norway, or a combination thereof. Thus, the barriers to gene flow that keep the Spitsbergen colonies distinct do not prevent the formation of a hybrid colony where individuals from the High Arctic and the cluster composed of mainland Norwegian, Icelandic and Faroese colonies meet.

The distinct population structure in the nuclear data is not observed in the mitochondrial genomes, which reveal an abundance of rare alleles and lack of significant population differentiation. The mitogenomic variation suggests that puffins experienced a recent population expansion, possibly out of a refugium after the Last Glacial Maximum. Indeed, it has been shown that mitogenomic variation in seabirds is dominated by

historical factors rather than representing contemporary gene flow⁴⁴, and a lack of mitogenomic population structure has been observed in many marine birds with high philopatry^{50,57,58}. In contrast to the mitogenomes, the structure in the nuclear data therefore likely originated after the last glacial period and reflects the influence of relatively recent barriers to gene flow in a context of historical demography^{15,44}. Such results are relevant for understanding the "seabird paradox", which contrasts the life-history traits of high philopatry and restricted dispersal in otherwise highly mobile species⁵⁹.

Our results have major implications for the conservation management of the Atlantic puffin. The genetic structure we identify in puffins disagrees with the suggestion of three subspecies (*F. a. naumanni*, *F. a. arctica*, *F. a. grabae*)³⁶. Although the genetically distinct Spitsbergen cluster coincides with the classification of morphologically large puffins in the High Arctic (*F. a. naumanni*)²⁸, we observe gene flow from Spitsbergen into Bjørnøya, which has been considered *F. a. arctica*²⁸. Furthermore, the geographic divide between *F. a. grabae* and *F. a. arctica* lies farther south than previously thought, with the Faroese puffins being genetically closer to *F. a. arctica* than to *F. a. grabae*. Nonetheless, *F. a. grabae* is currently represented by a single colony (Isle of May) in our study and the geographical extent of this genomic cluster needs to be refined by additional sampling, particularly in the western UK, Ireland, and France. Finally, puffins from the Western Atlantic region (e.g., colonies in Canada) form their own distinct genetic cluster that is not recognized within the current classification. Our results do not only warrant a revision of Salomonsen's taxonomic classification of three subspecies³⁶, but also highlight the need to acknowledge the four identified clusters as distinct units within the conservation management of puffins^{11,13,14}. Although puffin colonies within clusters are not genetically distinct entities, ecological independence illustrated by contrasting population dynamics across relatively small spatial scales (e.g., western Norway³¹) suggests that higher resolution local management units based on ecological differences should be considered. Nonetheless, the genetically distinct clusters at the outer edges of the puffin's distribution with putative local adaptations that will not be easily replenished indicate that conservation of these distinct clusters must be a first priority. Finally, our sampling does not cover several outskirts of the puffin's distribution, such as the U.S., northern Canada, Greenland, Ireland, western UK, France or Russia, and we may therefore still underestimate the true biological and genetic complexity of this species.

In conclusion, our study shows that a complex interplay of barriers to gene flow drives a previously unrecognized population diversification in the iconic Atlantic puffin. So far, much of seabird population genetics research has been based on mitochondrial and microsatellite data^{15,44}, which have limited power to characterize contemporary factors that determine population structure and gene flow^{20,60}. High-resolution nuclear data are therefore essential to help define evolutionary significant population units, disentangle convoluted ecological relationships, and are particularly important for seabird conservation, which aims to preserve genetic diversity considering profound global population declines^{7,8}, and the threat of global warming, which negatively impacts ecosystems worldwide⁶¹.

Methods

Ethical statement. Feather and blood samples of puffins included in this study were collected and handled under the following permits.

1. Gåsøyane, Røst, Hornøya, Bjørnøya (Norway)—FOTS ID #15602 and #15603 from the Norwegian Food Safety Authority for SEATRACK and SEAPOP; Permit 2018/607 from Miljødirektoratet (Norwegian Environment Agency), dated 4 May 2018.

- Gannet and Gull Island (Canada)—Canadian Wildlife Service Migratory Bird Banding Permit 10559 G, approved Animal Use Protocol (AUP) by Eastern Wildlife Animal Care Committee (17GR01, 18GR01), Newfoundland and Labrador Wilderness and Ecological Reserves Permit—Scientific Research (DOC/2017/02003), Canadian Wildlife Service Scientific Permit ST2785 (to M.L.M.), Canadian Wildlife Service Banding Permit 10694, and Acadia University Animal Care Committee Permits ACC 02-15 and 06-15 (to M.L.M.).
- Isle of May (Scotland)—Scottish Natural Heritage licence 2014/MON/RP/156 and Ringing Permit A400 (to MPH).
- Vestmannaeyjar, Papey, Breiðafjörður, Grimsey (Iceland)—Icelandic puffins were legally hunted during the hunting period of 1 July–15 August.
- Faroe—Feathers came from predated birds collected in the field after the predator was finished with them.

Draft reference genome assembly. A de novo Atlantic puffin draft genome was generated from the blood of a female Atlantic puffin. Read data were sequenced on three Illumina HiSeqX lanes using the 10x Genomics Chromium technology and assembled with the Supernova assembler (v2.1.1)⁶² after subsampling to 0.8 billion and 1 billion reads to maximize performance and remain within the computational capacity of the assembler. We refined the two assemblies through several steps, including merging of ‘haplotigs’, removal of contaminant sequences, misassembly correction, re-scaffolding using mapping coverage and linkage information, and gap filling (Supplementary Data 1a). The most complete and continuous 800 M and 1000 M assemblies together with the 3rd best assembly overall were selected for a second round of refinement (Supplementary Data 1b) resulting in a total of 72 draft assemblies. Of these, we kept the four most complete and continuous assemblies for additional gap filling and polishing, after which the most complete draft genome was selected for downstream analyses (Supplementary Data 1c). The puffin mitogenome was confidently identified by blasting (blastn) all scaffolds shorter than 25 kb against a custom-built database of 135 published mitogenomes of the order ‘Charadriiformes’ and annotated with the MITOS web server⁶³ (Fig. S1). The remaining nuclear scaffolds were ordered and concatenated into “pseudo-chromosomes” by mapping them to the razorbill genome (*Alca torda*—NCBI: bAlcTor1 primary, GCA_008658365.1) and applying 200 N’s as padding between each scaffold. We combined unmapped scaffolds into an “unplaced” pseudo-chromosome. We assessed the order and placement of scaffolds by investigating synteny in coverage and length between the puffin and razorbill chromosomes (Table S1). Details on the draft reference genome assembly and refinement can be found in the Supplementary File.

DNA extraction and sequencing. Samples from a total of 72 puffins collected across 12 breeding colonies (Fig. 1a) were made available for the present study by SEAPOP (<http://www.seapop.no/en>), SEATRACK (<http://www.seapop.no/en/seatrack>) and ARCTOX (<http://www.arctox.cnr.fr/en/home—Canadian> colonies). These samples had been collected between 2012 and 2018 and consisted of blood preserved in EtOH or lysis buffer, or feathers (Supplementary Data 2). We extracted DNA using the DNeasy Blood & Tissue kit (Qiagen) following the manufacturer’s protocol for animal blood or the nail/hair/feathers protocol applying several modifications for improved lysis and DNA yield. Individuals that had no sexing data associated with them were sexed using PCR amplification of specific allosome loci and visualization via gel electrophoresis. Genomic libraries were built by the Norwegian Sequencing Centre and sequenced on an Illumina HiSeq4000. We processed sequencing reads in PALEOMIX v1.2.14⁶⁴ and split the resulting bam files into nuclear and mitochondrial bam files. Additional details on the DNA extraction, sexing, sequencing and mapping are listed in the Supplementary File.

Mitogenome analyses. Genotypes across the mitochondrial genome were jointly called with GATK v4.1.4⁶⁵ by using the *HaplotypeCaller*, *CombineGVCFs*, and *GenotypeGVCFs* tool. We filtered genotypes according to GATKs Best Practices⁶⁶ and set genotypes with a read depth <3 or a quality <15 as missing. Indels and non-biallelic SNPs were removed and only SNPs present in all individuals were kept for subsequent analyses. The SNP dataset was annotated (Supplementary Data 3) with snpEff⁶⁷ utilizing the annotation of the newly assembled mitogenome of the Atlantic puffin and converted into a mitogenome sequence alignment. To serve as an outgroup, we appended four other species of the family Alcidae, i.e., the Razorbill (*Alca torda*, NCBI: CM018102.1), the Crested Auklet (*Aethia cristatella*, NCBI: NC_045517.1), the Ancient Murrelet (*Synthliboramphus antiquus*, NCBI: NC_007978.1) and the Japanese Murrelet (*Synthliboramphus wumizusume*, NCBI: NC_029328.1), to the alignment. To construct a maximum-likelihood phylogenetic tree, we split the alignment into seven partitions, i.e., one partition for a concatenated alignment of each of the three codon positions of the protein-coding genes, one partition for the concatenated alignment of the rRNA regions, one partition for the concatenated alignment of the tRNAs, one partition for the alignment of the control region, and one partition for the concatenated alignment of the “intergenic” regions. The best-fitting evolutionary model for each partition was found by *ModelFinder*⁶⁸ and the tree was built with IQTree v1.6.12⁶⁹ using 1000 ultrafast bootstrap replicates. We used the resulting tree to draw a haplotype genealogy graph with Fitch⁷⁰. Using Arlequin v.3.5⁷¹, we calculated haplotype (h),

nucleotide diversity (π), and Tajima’s D^{72} for each colony, for each genomic cluster defined by the nuclear analysis, and globally. In addition, an Ewens–Watterson test⁷³, Chakraborty’s test of population amalgamation⁷⁴, and Fu’s F_s test⁷⁵ were conducted for each of those groups. To further identify population differentiation, the proportion of sequence variation (Φ_{ST}) was estimated for all pairs of populations and genomic clusters. Hierarchical AMOVA tests subsequently determined the significance of a priori subdivisions into colonies and genomic clusters. Calculation of Φ_{ST} and AMOVA tests were also conducted in Arlequin. Additional details on the mitochondrial analyses are given in the Supplementary File.

Nuclear genome clustering and phylogenetic analyses. The majority of population genomic analyses were based on nuclear genotype likelihoods as implemented in ANGSD v.0.931⁷⁶. After assessing the quality of the mapped sequencing data in an ANGSD pre-run, we removed an individual from the Isle of May from the dataset. Genotype likelihoods for nuclear SNPs covered in all individuals were calculated and filtered in ANGSD. Accounting for linkage disequilibrium, we further pruned the dataset by only selecting the most central site within blocks of linked sites ($R^2 > 0.2$) as in Orlando and Librado⁷⁷. Subsequently, all variants located on the Z-pseudo-chromosome and “unplaced scaffolds” were excluded from the analyses yielding a final genotype likelihood panel consisting of 1,093,765 sites. We investigated genomic population structure with a PCA of the genotype likelihood panel using PCAngsd v0.982⁷⁸. Individual ancestry proportions were estimated using a maximum likelihood (ML) approach implemented in ngsAdmix v32⁷⁹, with the number of ancestral populations (K) set from 1 to 10 and conducting 50 replicate runs for each K. The runs were clustered after similarity for each K and ancestry proportions were averaged within the major cluster using Clumpak⁸⁰ with default settings. Additional “hierarchical” PCA and admixture analyses were conducted for genomic sub-cluster(s) using identical methods.

After adding the razorbill genome as an outgroup to the genotype likelihood panel by mapping unpublished, raw 10x Genomics sequencing data used for the assembly of the embargoed razorbill genome to the puffin draft assembly, we built a neighbor-joining (NJ) tree based on pairwise genetic distance matrices (p-distance) and a sample-based ML phylogenetic tree in FastMe v2.1.5⁸¹ and Treemix v1.13⁸², respectively. For both trees, 100 bootstrap replicates were generated. To infer patterns of population splitting and mixing, we produced population-based ML trees including up to ten migration edges. The optimal number of migrations was selected using a quantitative approach by evaluating the distribution of explained variance, the log likelihoods, the covariance with an increase in migration edges, and by applying the method of Evanno⁴¹ and several different linear threshold models. The topology for m_0 and m_{BEST} was evaluated by generating 100 bootstrap replicates. Additional details on the cluster and phylogenetic analyses are given in the Supplementary File.

Genetic diversity, heterozygosity, and inbreeding. We calculated a set of neutrality tests and population statistics in ANGSD using colony-based one-dimensional (1D) folded site frequency spectra (SFS). For each population, genomic cluster, and globally, Tajima’s D and nucleotide diversity (π) were computed utilizing the per-site θ estimates. Individual genome-wide heterozygosity was calculated in ANGSD using individual, folded, 1D SFS. We calculated heterozygosity by dividing the number of polymorphic sites by the number of total sites present in the SFS.

The proportion of RoH within each puffin genome was computed by calculating local estimates of heterozygosity in 100 kb sliding windows (50 kb slide) following the approach in Sánchez-Barreiro et al.⁴². We defined the 10% quantile of the average local heterozygosity across all samples as the cutoff for a “low heterozygosity region” (Fig. S18). RoHs were declared as all regions with at least two subsequent windows of low heterozygosity (below cutoff) and their final length was calculated as described in Sánchez-Barreiro et al.⁴². We calculated an individual inbreeding coefficient based on the RoH, F_{RoH} , as in Sánchez-Barreiro et al.⁴² by computing the fraction of the entire genome falling into RoHs, with the entire genome being the total length of windows scanned. Additional details on these analyses can be found in the Supplementary File.

Patterns of gene flow and admixture. Assessing potential patterns of IBD within the breeding range of the puffin, the program EEMS⁴³ was used to model the association between genetic and geographic data by visualizing the existing population structure and highlighting regions of higher-than-average and lower-than-average historic gene flow. We calculated a pairwise genetic distance matrix in ANGSD by sampling the consensus base (*-doIBS 2 -makeMatrix 1*) at the sites included in the genotype likelihood set (see *Nuclear cluster and phylogenetic analyses*) for each sample. The matrix was fed into 10 independent runs of EEMS, each consisting of one MCMC chain of six million iterations with a two million iteration burn-in, 9999 thinning iterations, and 1000 underlying demes.

Supplementing the results of the EEMS analysis, we conducted a traditional IBD analysis by determining geographical and genetic distances between the 12 colonies and assessing the significance of the correlation between the two distance matrices with a Mantel test⁸³ and a multiple regression on distance matrix (MRM)⁸⁴ analysis. F_{ST} was used as a proxy for genetic distance and computed for each population pair in ANGSD by applying two-dimensional (2D), folded SFS. We converted pairwise F_{ST} values to Slatkin’s linearized F_{ST} ⁸⁵. Least Cost Path distances (paths over water only) between colony coordinates (latitude/longitude)

were calculated using the R package *marmap*⁸⁶ and used as geographic distances. We performed the Mantel test (999 permutations) and MRM analysis with the R package *ecodist*⁸⁷. All analyses for IBD were re-run on subsets of colonies by progressively removing the colony from the geographic and genetic distance matrices, whose removal led to the highest increase in the proportion of variance in genetic distance explained by geographic distance in the resulting regression model (Spitsbergen, Isle of May, Bjørnøya and Gannet Isl.).

A distance-based Redundancy Analysis (dbRDA)⁸⁸ was conducted to corroborate the results of the MRM analyses and Mantel tests and to estimate the relative contribution of IBD and IBE to the observed Atlantic puffin population structure. The dbRDA was run between the genetic distance matrix versus geographic and environmental parameters⁸⁸. A global dbRDA was performed with all geographic and environmental variables, and for statistically significant global dbRDA models, the most significant variables (geographic or environmental) were selected via a stepwise regression⁸⁹. Those served as input for a reduced dbRDA to calculate the marginal effect of each variable and for a partial dbRDA with variance partitioning to estimate the separate effects of IBD and IBE. Similar to the MRM analyses and Mantel tests, these analyses were repeated on subsets of colonies by progressively removing the colony from the geographic, environmental, and genetic distance matrices, whose removal led to the highest increase in variance explained in the resulting global dbRDA model. Methods and R code for the dbRDA were found at <https://github.com/laurabenestan/db-RDA-and-db-MEM>⁹⁰.

Additional assessments of gene flow and admixture were conducted by calculating f_3 -statistics and multi-population D-statistics (aka ABBA BABA test)⁹¹. We calculated f_3 -statistics in Treemix for each unique combination of ((A,B),C) of the 12 puffin populations. D-statistics were calculated in ANGSD (-doAbbababa2) for each combination of ((A,B),C), Outgroup) using the 12 puffin colonies. The outgroup was generated in ANGSD using the 10xGenomics sequencing data of the razorbill mapped to the puffin reference genome (see *Nuclear cluster and phylogenetic analyses*).

Evaluating genome-wide patterns of genetic differentiation, pairwise F_{ST} values between the Norway/Iceland/Faroe cluster and the Spitsbergen, Isle of May, Canada colonies (three comparisons) were calculated in sliding windows of 50 kb with 12.5 kb steps across the 25 pseudo-chromosomes by applying 2D, folded SFS. The window size of 50 kb was chosen for sliding window analyses because LD decays to ca. 10% ($R < 0.025$) within this distance (Fig. S19). Additional details on the IBD, admixture, and sliding-window analyses are given in the Supplementary File.

Statistics and reproducibility. The research sample included 72 adult Atlantic puffins (*Fratercula arctica*) across 12 colonies located in Svalbard, northern mainland Norway, Iceland, the Faroe Islands, Scotland, and Canada. The sample included six individuals per colony (12 colonies), including an equal sex ratio (3 males and 3 females per colony). All statistical tests were conducted using publicly available programs and packages as described in the methodological sections above. Reproducibility can be accomplished by following the sample collection and laboratory methods outlined above and by following the author's GitHub (<https://github.com/OKersten/PuffPopGen>) using the specified parameters mentioned in the code and methodological sections above.

Reporting summary. Further information on research design is available in the Nature Research Reporting Summary linked to this article.

Data availability

Raw read data analyzed in the current study have been deposited in the European Nucleotide Archive (ENA, www.ebi.ac.uk/ena) under study accession number PRJEB40631 (see Supplementary Data 2 for individual sample accession numbers). Nuclear and mitochondrial scaffolds (GCA_905066775.1, CAJHIB01000001-CAJHIB010013329), as well as pseudo-chromosomes (GCA_905066775.2, CAJHIB02000001-CAJHIB020000027), have been uploaded to ENA (Project PRJEB40926, Sample SAMEA7482542).

Code availability

Full code used for the population genomic analyses is available on the first author's GitHub (<https://github.com/OKersten/PuffPopGen>) and on Zenodo under the <https://doi.org/10.5281/zenodo.4899574>⁹². This includes versions of any software used, if relevant, and any specific variables or parameters used to generate, test, and process the dataset of this study.

Received: 17 November 2020; Accepted: 1 July 2021;

Published online: 29 July 2021

References

- Otero, X. L., De La Peña-Lastra, S., Pérez-Alberti, A., Ferreira, T. O. & Huerta-Díaz, M. A. Seabird colonies as important global drivers in the nitrogen and phosphorus cycles. *Nat. Commun.* **9**, 246 (2018).
- Velarde, E., Anderson, D. W. & Ezcurra, E. Seabird clues to ecosystem health. *Science* **365**, 116–117 (2019).
- Piatt, J. F., Sydeman, W. J. & Wiese, F. Introduction: a modern role for seabirds as indicators. *Mar. Ecol. Prog. Ser.* **352**, 199–204 (2007).
- Boersma, P. D., Clark, J. A. & Hillgarth, N. Seabird conservation. In *Biology of Marine Birds* (eds. Schreiber, E. & Burger, J.) 559–579 (CRC Press Boca Raton, 2002).
- Denlinger, L. & Wohl, K. Seabird harvest regimes in the circumpolar nations. *Conservation of Arctic Flora and Fauna (CAFF)*, (2001).
- Merkel, F. & Barry, T. Seabird Harvest in the Arctic. *Conservation of Arctic Flora and Fauna (CAFF)*, (2008).
- Croxall, J. P. et al. Seabird conservation status, threats and priority actions: a global assessment. *Bird. Conserv. Int.* **22**, 1–34 (2012).
- Palczy, M., Hammill, E., Karpouz, V. & Pauly, D. Population trend of the world's monitored seabirds, 1950–2010. *PLoS ONE* **10**, e0129342 (2015).
- Frederiksen, M. Seabirds in the North East Atlantic. Summary of status, trends and anthropogenic impact. *TemaNord* **587**, 21–24 (2010).
- Chardine, J. & Mendenhall, V. Human Disturbance at Arctic Seabird Colonies. *Conservation of Arctic Flora and Fauna (CAFF)*, (1998).
- Funk, W. C., McKay, J. K., Hohenlohe, P. A. & Allendorf, F. W. Harnessing genomics for delineating conservation units. *Trends Ecol. Evol.* **27**, 489–496 (2012).
- Moritz, C. Defining 'Evolutionarily Significant Units' for conservation. *Trends Ecol. Evol.* **9**, 373–375 (1994).
- Allendorf, F. W., Hohenlohe, P. A. & Luikart, G. Genomics and the future of conservation genetics. *Nat. Rev. Genet.* **11**, 697 (2010).
- Fraser, D. J. & Bernatchez, L. Adaptive evolutionary conservation: towards a unified concept for defining conservation units. *Mol. Ecol.* **10**, 2741–2752 (2001).
- Friesen, V. L. Speciation in seabirds: why are there so many species... and why aren't there more? *J. Ornithol.* **156**, 27–39 (2015).
- Taylor, R. S. et al. Sympatric population divergence within a highly pelagic seabird species complex (*Hydrobates* spp.). *J. Avian Biol.* **49**, 1–14 (2018).
- Rexer-Huber, K. et al. Genomics detects population structure within and between ocean basins in a circumpolar seabird: the white-chinned petrel. *Mol. Ecol.* **28**, 4552–4572 (2019).
- Clucas, G. V. et al. Comparative population genomics reveals key barriers to dispersal in Southern Ocean penguins. *Mol. Ecol.* **27**, 4680–4697 (2018).
- Frugone, M. J. et al. More than the eye can see: Genomic insights into the drivers of genetic differentiation in Royal/Macaroni penguins across the Southern Ocean. *Mol. Phylogenet. Evol.* **139**, 106563 (2019).
- Cristofari, R. et al. Unexpected population fragmentation in an endangered seabird: the case of the Peruvian diving-petrel. *Sci. Rep.* **9**, 2021 (2019).
- Tigano, A., Shultz, A. J., Edwards, S. V., Robertson, G. J. & Friesen, V. L. Outlier analyses to test for local adaptation to breeding grounds in a migratory arctic seabird. *Ecol. Evol.* **7**, 2370–2381 (2017).
- Lowry, D. B. et al. Breaking RAD: an evaluation of the utility of restriction site-associated DNA sequencing for genome scans of adaptation. *Mol. Ecol. Resour.* **17**, 142–152 (2017).
- Somvichian-Clausen, A. Behind the stunning photo of a puffin gorging on fish. *Natl Geographic* (2017).
- Huijbens, E. H. & Einarsson, N. Feasting on Friends: Whales, Puffins, and Tourism in Iceland. In *Tourism Experiences and Animal Consumption* (ed. Kline, C.) 10–27 (Routledge, 2018).
- Lund, K. A., Kjartansdóttir, K. & Loftsdóttir, K. 'Puffin love': performing and creating Arctic landscapes in Iceland through souvenirs. *Tour. Stud.* **18**, 142–158 (2018).
- Hodgetts, L. M. Animal bones and human society in the late younger stone age of arctic Norway. (Durham University, 1999).
- Dove, C. J. & Wickler, S. Identification of bird species used to make a Viking age feather pillow. *Arctic* **69**, 29–36 (2016).
- Harris, M. P. & Wanless, S. The puffin (T & AD Poyser, Bloomsbury Publishing, 2011).
- BirdLife International. *Fratercula arctica*. The IUCN Red List of Threatened Species 2017 (2017)
- Anker-Nilssen, T. & Aarvak, T. The population ecology of puffins at Røst. Status after the breeding season 2001. *NINA Oppdragsmeld.* **736**, 1–40 (2002).
- Anker-Nilssen, T. et al. Key-site monitoring in Norway 2019, including Svalbard and Jan Mayen. SEAPOP Short Report 1–2020 (2020).
- Lilliendahl, K. et al. Recruitment failure of Atlantic puffins *Fratercula arctica* and sandeels *Ammodytes marinus* in Vestmannaeyjar Islands. *N. áttúrufræðingurinn* **83**, 65–79 (2013).
- Walker, S. J. & Meijer, H. J. M. Size variation in mid-Holocene North Atlantic Puffins indicates a dynamic response to climate change. *PLoS ONE* **16**, e0246888 (2021).
- Burnham, K. K., Burnham, J. L. & Johnson, J. A. Morphological measurements of Atlantic puffin (*Fratercula arctica naumanni*) in High-Arctic Greenland. *Polar Res.* **39**. <https://doi.org/10.33265/polar.v39.5242> (2020).

35. Gaston, A. J. & Provencher, J. F. A specimen of the high arctic subspecies of Atlantic Puffin, *Fratercula arctica naumanni*, in Canada. *Can. Field-Nat.* **126**, 50–54 (2012).
36. Salomonsen, F. *The Atlantic Alcidae*. vol. 6 (Elanders boktryckeri aktiebolag, 1944).
37. Moen, S. M. Morphologic and genetic variation among breeding colonies of the Atlantic puffin (*Fratercula arctica*). *Auk* **108**, 755–763 (1991).
38. Harris, M. P. Measurements and weights of British Puffins. *Bird. Study* **26**, 179–186 (1979).
39. Kim, J. A., Kang, S.-G., Yang, J. W., Hur, W.-H. & Kil, H.-J. Complete mitochondrial genome of *Aethia cristatella* (Charadriiformes: Alcidae). *Mitochondrial DNA Part B* **5**, 31–32 (2020).
40. Eo, S. H. & An, J. The complete mitochondrial genome sequence of Japanese murrelet (*Aves: Alcidae*) and its phylogenetic position in Charadriiformes. *Mitochondrial DNA A DNA Mapp. Seq. Anal.* **27**, 4574–4575 (2016).
41. Evanno, G., Regnaut, S. & Goudet, J. Detecting the number of clusters of individuals using the software STRUCTURE: a simulation study. *Mol. Ecol.* **14**, 2611–2620 (2005).
42. Sánchez-Barreiro, F. et al. Historical Population Declines Prompted Significant Genomic Erosion in the Northern and Southern White Rhinoceros (*Ceratotherium Simum*). *Molecular Ecology*. 1–15 <https://doi.org/10.1111/mec.16043> (2021).
43. Petkova, D., Novembre, J. & Stephens, M. Visualizing spatial population structure with estimated effective migration surfaces. *Nat. Genet.* **48**, 94–100 (2016).
44. Lombal, A. J., O'dwyer, J. E., Friesen, V., Woehler, E. J. & Burridge, C. P. Identifying mechanisms of genetic differentiation among populations in vagile species: historical factors dominate genetic differentiation in seabirds. *Biol. Rev. Camb. Philos. Soc.* **95**, 625–651 (2020).
45. Friesen, V. L., Burg, T. M. & McCoy, K. D. Mechanisms of population differentiation in seabirds. *Mol. Ecol.* **16**, 1765–1785 (2007).
46. Breton, A. R., Diamond, A. W. & Kress, S. W. Encounter, survival, and movement probabilities from an Atlantic puffin (*Fratercula arctica*) metapopulation. *Ecol. Monogr.* **75**, 133–149 (2006).
47. Fayet, A. L. et al. Ocean-wide drivers of migration strategies and their influence on population breeding performance in a declining seabird. *Curr. Biol.* **27**, 3871–3878.e3 (2017).
48. Burg, T. M. & Croxall, J. P. Global relationships amongst black-browed and grey-headed albatrosses: analysis of population structure using mitochondrial DNA and microsatellites. *Mol. Ecol.* **10**, 2647–2660 (2001).
49. Lowther, P. E., Diamond, T., Kress, S. W., Robertson, G. J. & Gill, F. Atlantic Puffin (*Fratercula arctica*). The Birds of North America Online 18, (2002).
50. Wojczulanis-Jakubas, K. et al. Weak population genetic differentiation in the most numerous Arctic seabird, the little auk. *Polar Biol.* **37**, 621–630 (2014).
51. Smith, A. L., Monteiro, L., Hasegawa, O. & Friesen, V. L. Global phylogeography of the band-rumped storm-petrel (*Oceanodroma castro*; Procellariiformes: Hydrobatidae). *Mol. Phylogenet. Evol.* **43**, 755–773 (2007).
52. Bergmann, C. Über die Verhältnisse der Wärmeökonomie der Tiere zu ihrer Grösse. *Göttinger Stud.* **3**, 595–708 (1847).
53. James, F. C. Geographic size variation in birds and its relationship to climate. *Ecology* **51**, 365–390 (1970).
54. Yamamoto, T. et al. Geographical variation in body size of a pelagic seabird, the streaked shearwater *Calonectris leucomelas*. *J. Biogeogr.* **43**, 801–808 (2016).
55. Barrett, R. T., Anker-Nilssen, T. & Krasnov, Y. V. Can Norwegian and Russian razorbills (*Alca torda*) be identified by their measurements? *Mar. Ornithol.* **25**, 5–8 (1997).
56. Anker-Nilssen, T., Aarvak, T. & Bangjord, G. Mass mortality of Atlantic Puffins *Fratercula arctica* off Central Norway, spring 2002: causes and consequences. *Atl. Seab.* **5**, 57–72 (2003).
57. Pearce, R. L. et al. Mitochondrial DNA suggests high gene flow in ancient murrelets. *Condor* **104**, 84–91 (2002).
58. Thomas, J. E. et al. Demographic reconstruction from ancient DNA supports rapid extinction of the great auk. *eLife* **8**, e47509 (2019).
59. Milot, E., Weimerskirch, H. & Bernatchez, L. The seabird paradox: dispersal, genetic structure and population dynamics in a highly mobile, but philopatric albatross species. *Mol. Ecol.* **17**, 1658–1673 (2008).
60. Edwards, S. & Bensch, S. Looking forwards or looking backwards in avian phylogeography? A comment on Zink and Barrowclough 2008. *Mol. Ecol.* **18**, 2930–2936 (2009).
61. IPCC. Global Warming of 1.5 °C—Summary for Policy Makers. (2018).
62. Weisenfeld, N. L., Kumar, V., Shah, P., Church, D. M. & Jaffe, D. B. Direct determination of diploid genome sequences. *Genome Res.* **27**, 757–767 (2017).
63. Bernt, M. et al. MITOS: improved de novo metazoan mitochondrial genome annotation. *Mol. Phylogenet. Evol.* **69**, 313–319 (2013).
64. Schubert, M. et al. Characterization of ancient and modern genomes by SNP detection and phylogenomic and metagenomic analysis using PALEOMIX. *Nat. Protoc.* **9**, 1056–1082 (2014).
65. McKenna, A. et al. The Genome Analysis Toolkit: a MapReduce framework for analyzing next-generation DNA sequencing data. *Genome Res.* **20**, 1297–1303 (2010).
66. Van der Auwera, G. A. et al. From FastQ data to high confidence variant calls: the Genome Analysis Toolkit best practices pipeline. *Curr. Protoc. Bioinforma.* **43**, 11.10.1–33 (2013).
67. Cingolani, P. et al. A program for annotating and predicting the effects of single nucleotide polymorphisms, SnpEff: SNPs in the genome of *Drosophila melanogaster* strain w1118; iso-2; iso-3. *Fly* **6**, 80–92 (2012).
68. Kalyaanamoorthy, S., Minh, B. Q., Wong, T. K. F., von Haeseler, A. & Jermini, L. S. ModelFinder: fast model selection for accurate phylogenetic estimates. *Nat. Methods* **14**, 587–589 (2017).
69. Nguyen, L.-T., Schmidt, H. A., von Haeseler, A. & Minh, B. Q. IQ-TREE: a fast and effective stochastic algorithm for estimating maximum-likelihood phylogenies. *Mol. Biol. Evol.* **32**, 268–274 (2015).
70. Mutschiner, M. Fitchi: haplotype genealogy graphs based on the Fitch algorithm. *Bioinformatics* **32**, 1250–1252 (2016).
71. Excoffier, L. & Lischer, H. E. L. Arlequin suite ver 3.5: a new series of programs to perform population genetics analyses under Linux and Windows. *Mol. Ecol. Resour.* **10**, 564–567 (2010).
72. Tajima, F. Statistical method for testing the neutral mutation hypothesis by DNA polymorphism. *Genetics* **123**, 585–595 (1989).
73. Watterson, G. A. Heterosis or neutrality? *Genetics* **85**, 789–814 (1977).
74. Chakraborty, R. & Mitochondrial, D. N. A. polymorphism reveals hidden heterogeneity within some Asian populations. *Am. J. Hum. Genet.* **47**, 87–94 (1990).
75. Fu, Y. X. Statistical tests of neutrality of mutations against population growth, hitchhiking and background selection. *Genetics* **147**, 915–925 (1997).
76. Korneliusen, T. S., Albrechtsen, A. & Nielsen, R. ANGSD: analysis of next generation sequencing data. *BMC Bioinforma.* **15**, 356 (2014).
77. Orlando, L. & Librado, P. Origin and evolution of deleterious mutations in horses. *Genes* **10**, 649 (2019).
78. Meisner, J. & Albrechtsen, A. Inferring population structure and admixture proportions in low-depth NGS data. *Genetics* **210**, 719–731 (2018).
79. Skotte, L., Korneliusen, T. S. & Albrechtsen, A. Estimating individual admixture proportions from next generation sequencing data. *Genetics* **195**, 693–702 (2013).
80. Kopelman, N. M., Mayzel, J., Jakobsson, M., Rosenberg, N. A. & Mayrose, I. Clumpak: a program for identifying clustering modes and packaging population structure inferences across K. *Mol. Ecol. Resour.* **15**, 1179–1191 (2015).
81. Lefort, V., Desper, R. & Gascuel, O. FastME 2.0: a comprehensive, accurate, and fast distance-based phylogeny inference program. *Mol. Biol. Evol.* **32**, 2798–2800 (2015).
82. Pickrell, J. K. & Pritchard, J. K. Inference of population splits and mixtures from genome-wide allele frequency data. *PLoS Genet.* **8**, e1002967 (2012).
83. Mantel, N. The detection of disease clustering and a generalized regression approach. *Cancer Res.* **27**, 209–220 (1967).
84. Lichstein, J. W. Multiple regression on distance matrices: a multivariate spatial analysis tool. *Plant Ecol.* **188**, 117–131 (2007).
85. Slatkin, M. A measure of population subdivision based on microsatellite allele frequencies. *Genetics* **139**, 457–462 (1995).
86. Pante, E., Simon-Bouhet, B. & Irissou, J.-O. *marmar—R package*. (2019).
87. Goslee, S. & Urban, D. The ecodist package for dissimilarity-based analysis of ecological data. *J. Stat. Softw., Artic.* **22**, 1–19 (2007).
88. Legendre, P. & Anderson, M. J. Distance-based redundancy analysis: testing multispecies responses in multifactorial ecological experiments. *Ecol. Monogr.* **69**, 1–24 (1999).
89. Blanchet, F. G., Legendre, P. & Borcard, D. Modelling directional spatial processes in ecological data. *Ecol. Modell.* **215**, 325–336 (2008).
90. Benestan, L. M. et al. Population genomics and history of speciation reveal fishery management gaps in two related redfish species (*Sebastes mentella* and *Sebastes fasciatus*). *Evol. Appl.* **14**, 588–606 (2021).
91. Soraggi, S., Wiuf, C. & Albrechtsen, A. Powerful inference with the D-statistic on low-coverage whole-genome data. *G3* **8**, 551–566 (2018).
92. Kersten, O. Code for Population Genomics Analyses of Atlantic Puffin (*Fratercula arctica*) using Whole Genome Sequencing (Version v1.0). Zenodo. <https://doi.org/10.5281/zenodo.4899575> (2021).

Acknowledgements

Financial support was provided by the Nansen Foundation and the Faculty of Mathematical and Natural Sciences, University of Oslo (UiO). We are grateful to the SEAPOP program (www.seapop.no/en), Norwegian Research Council grant number 192141), and the SEATRACK (<http://www.seapop.no/en/seatrack>) and ARCTOX (<https://arctox.cnrs>).

[fr/en/home](#)) projects for collecting and sharing of samples. In particular, we thank Dave Fifield and Greg Robertson for the provision of puffin samples from Gull Island, and Árni Ásgeirsson and Róbert Arnar Stefánsson for supplying samples from Breiðafjörður. The authors acknowledge support from the National Genomics Infrastructure in Stockholm funded by the Science for Life Laboratory, the Knut and Alice Wallenberg Foundation and the Swedish Research Council, and the SNIC/Uppsala Multidisciplinary Center for Advanced Computational Science for assistance with massively parallel sequencing (reference genome) and access to the UPPMAX computational infrastructure. Special thanks goes to the Norwegian Sequencing Centre, UiO (<https://www.sequencing.uio.no>) for the genomic libraries and resequencing of samples analyzed in this study. The razorbill genome data was made available for this study by Tom Gilbert and the Vertebrate Genome Project. Computation was performed using the resources and assistance from SIGMA2. Albína Pálsdóttir shared scripts for ANGSD, and Emiliano Trucchi advised on the manuscript. Pictures of puffins used in the figures were taken by Annemarie Look.

Author contributions

S.B. and B.S. conceptualized the project. M.I. performed the DNA extraction for the reference genome. O.K. did all other laboratory work. K.S.J. advised on the sequencing strategy and co-supervised O.K. O.K. refined the reference genome assembly. O.K. carried out the population genomic analyses with input from S.B., B.S., and D.M.L. O.K. designed the figures with input from S.B., B.S., and D.M.L. T.A.N., H.S., and E.S.H. advised on colony selection and provided ecological context. T.A.N., H.S., O.K., S.D., E.S.H., J.F., M.P.H., J.D., K.E., M.L.M., and M.G.F. provided samples. O.K. wrote the paper with S.B., B.S., and D.M.L. All authors read and revised the final version of the manuscript.

Competing interests

The authors declare no competing interests.

Additional information

Supplementary information The online version contains supplementary material available at <https://doi.org/10.1038/s42003-021-02415-4>.

Correspondence and requests for materials should be addressed to O.K. or S.B.

Peer review information *Communications Biology* thanks the anonymous reviewers for their contribution to the peer review of this work. Primary Handling Editor: Caitlin Karniski.

Reprints and permission information is available at <http://www.nature.com/reprints>

Publisher's note Springer Nature remains neutral with regard to jurisdictional claims in published maps and institutional affiliations.



Open Access This article is licensed under a Creative Commons Attribution 4.0 International License, which permits use, sharing, adaptation, distribution and reproduction in any medium or format, as long as you give appropriate credit to the original author(s) and the source, provide a link to the Creative Commons license, and indicate if changes were made. The images or other third party material in this article are included in the article's Creative Commons license, unless indicated otherwise in a credit line to the material. If material is not included in the article's Creative Commons license and your intended use is not permitted by statutory regulation or exceeds the permitted use, you will need to obtain permission directly from the copyright holder. To view a copy of this license, visit <http://creativecommons.org/licenses/by/4.0/>.

© The Author(s) 2021